Electric-Field-Induced Structural and Electronic Changes and Decomposition of Crystalline Lead Azide: A Computational Study

ARTICLE *in* THE JOURNAL OF PHYSICAL CHEMISTRY C · APRIL 2015

Impact Factor: 4.77 · DOI: 10.1021/jp507822z

6 AUTHORS, INCLUDING:

Zhimin Li
The Hong Kong University of Science and Tec…
39 PUBLICATIONS **167** CITATIONS
SEE PROFILE

Huisheng Huang
18 PUBLICATIONS **65** CITATIONS
SEE PROFILE

Jian-Guo Zhang
Beijing Institute of Technology
312 PUBLICATIONS **1,579** CITATIONS
SEE PROFILE

Li Yang
Nanjing Medical University
155 PUBLICATIONS **1,621** CITATIONS
SEE PROFILE

THE JOURNAL OF PHYSICAL CHEMISTRY C

Article

pubs.acs.org/JPCC

Electric-Field-Induced Structural and Electronic Changes and Decomposition of Crystalline Lead Azide: A Computational Study

Zhimin Li,[†,‡,∥] Huisheng Huang,*[,§,∥] Tonglai Zhang,*[,†] Jianhua Xu,[§] Jianguo Zhang,[†] and Li Yang[†]

[†]State Key Laboratory of Explosion Science and Technology, Beijing Institute of Technology, 5 South Zhongguancun Street, Haidian District, Beijing 100081, China

[‡]Beijing Key Laboratory of Ionic Liquids Clean Process, State Key Laboratory of Multiphase Complex Systems, Institute of Process Engineering, Chinese Academy of Sciences, 1 North 2nd Street, Zhongguancun, Haidian District, Beijing 100190, China

[§]Chongqing Key Laboratory of Inorganic Special Functional Materials, College of Chemistry and Chemical Engineering, Yangtze Normal University, 98 Julong Road, Lidu Fuling District, Chongqing 408100, China

ABSTRACT: Periodic first-principles calculations have been performed to study the effects of electric field on the geometric and electronic structures and decomposition mechanism of crystalline lead azide (α-$Pb(N_3)_2$). The results show that the influence of external electric field on the crystal structure is anisotropic owing to the different crystal packing along three crystallographic directions. The applied field causes a little change in unit cell volume, and the crystal symmetry remains unchanged, indicating that lead azide does not undergo a phase transition at an applied field smaller than 8.017 V/nm. The electric field effects on the ionic Pb−N bonds are stronger than those on the covalent N−N bonds because more effective charges reside on the atoms in the former. Moreover, the applied field across the crystal develops instabilities. The Franz−Keldysh effect yields larger influence on the band gap than the structural change induced by applied field. At the field higher than 4.453 V/nm, lead azide has metallic properties. Additionally, lead azide is more sensitive to external electric field than lead styphnate. Although the electric field redistributes the electron density of the frontier molecular orbitals, the decomposition mechanism of lead azide in the presence and absence of the field is similar. Finally, the electric-field-induced decomposition of lead azide produces N_2 and metallic lead.

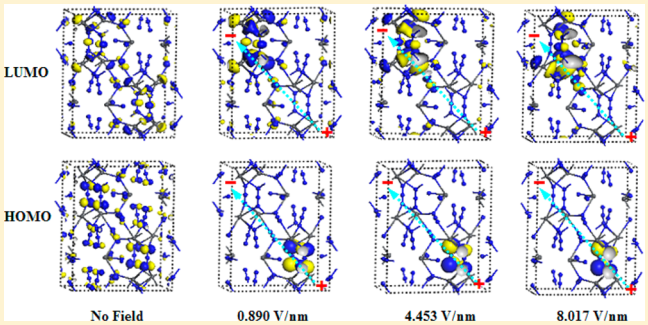

1. INTRODUCTION

When an electric field is applied on the bulk material, there are variations in the band structure, and the effective band gap is reduced, consequently leading to the changes in optical absorption edge and refractive index. This is the so-called Franz−Keldysh effect (FKE), which is utilized in electro-absorption modulators.[1,2] Furthermore, some materials can spontaneously break at a sufficiently high applied field. For instance, the decomposition reaction of energetic materials can be triggered by not only impact, friction, heat, and static compression but also external electric field. The influences of temperature and pressure on the structure and properties of explosives have been fully studied theoretically and experimentally;[3−12] however, except for lead styphnate,[13] theoretical investigations on energetic solids under external electric field have not been made, although the hazards of energetic materials owing to static charge have been extensively studied experimentally.[14−18] The electrostatic discharge hazard is normally associated with manufacturing and filling operations, and the discharge of static electricity accumulated on a person can supply energy up to 20 mJ, which is possibly bigger than the minimum spark energy required for initiating the energetic materials such as lead styphnate and basic lead azide.[16] Hence, an accident resulting from static charge can easily occur in an explosive production plant. Moreover, the electric spark sensitivity of various explosives has been the subject of many articles in the literature.[19−31] The correlations between the spark sensitivity of explosives and their molecular electronic properties have been well established, while the external electric-field influences on the structure and properties of energetic materials are still not well understood.

It is known that lead azide is a typical primary explosive and has been extensively used for a long time. Thereby, its structure, thermal decomposition, and sensitivity and optical properties are fully investigated and compared.[32−34] Also, there are a few experimental studies of the dielectric breakdown of lead azide.[35,36] Unfortunately, the geometric and electronic structures and decomposition mechanism under external electric field are often difficult to obtain from experiment for practical reasons. Compared with experiment, simulation can provide more detailed information about variations in crystal and molecular structures, initiation mechanism, and stability of energetic

Received: August 3, 2014
Revised: March 3, 2015
Published: April 2, 2015

DOI: 10.1021/jp507822z
J. Phys. Chem. C 2015, 119, 8431−8437

materials under applied electric field. In fact, there are sufficient computational investigations on the structures and properties of materials including single-walled nanotubes,[37−39] graphene nanoribbons,[40] guanine aggregates,[41] carbon dioxide,[42] and lead styphnate[13] under external electric field. To the best of our knowledge, there are no such reports on lead azide. Thus, in the present work, periodic first-principles calculations have been performed using density functional theory to study the effects of electric field on the geometric and electronic structures, decomposition mechanism, and stability of crystalline lead azide.

2. COMPUTATIONAL METHOD

The initial structure adopted the experimental crystalline structure[32] in which lead azide contains 12 $Pb(N_3)_2$ molecules per unit cell in an orthorhombic lattice with space group *Pnma*, as shown in Figure 1. The geometry optimization was performed to allow the ionic configuration, cell shape, and volume to change. The total energy of the system was converged <1.0×10^{-5} Ha, the residual force <0.002 Ha/Å, and the displacement of atoms <0.005 Å. Some previous theoretical studies[34,43] show that the generalized gradient approximation (GGA) proposed by Perdew and Wang,[44] named PW91, can better reproduce the crystal structures of metal azides. Additionally, their band gaps and density of states (DOS) calculated by the PW91 functional are reasonably satisfactory. Therefore, the PW91 functional was employed in the present work.

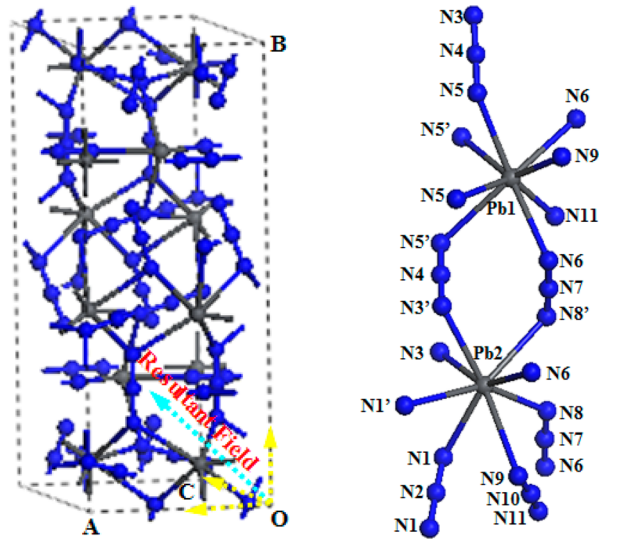

Figure 1. Experimental unit cell of lead azide and the orientations of the resultant applied field (green arrow) and its *a*, *b*, and *c* components (yellow arrows) and atomic numbering of the Pb ions and their neighboring N atoms and azide ions.

In the geometry relaxation and electronic structure calculation, the effective core potentials, double numerical polarization (DNP) basis set, global orbital cutoff scheme, and direct inversion in an iterative subspace (DIIS) were used. The self-consistent field (SCF) tolerance was 1.0×10^{-6} Ha. Moreover, Brillouin zone sampling was performed by using the Monkhorst−Pack scheme. Our test calculations suggest that the computed structural parameters are not sensitive to the *k*-point sampling, and reasonable accuracy could be obtained by performing each optimization using a $(1 \times 1 \times 1)$ sampling grid. The band gap and density of states of the optimized structures were then determined using the $(4 \times 2 \times 2)$ *k*-point sampling grid.

The influence of the external electric field on the structural and electronic properties of crystalline lead azide was systematically investigated. In the calculation, the electric field is described in terms of the *a*, *b*, and *c* components. Thereby, the static external electric fields are separately applied in the *a*, *b*, and *c* directions. The real strength and orientation of the applied field should be expressed in their resultant vector, as displayed in Figure 1. The measured room-temperature breakdown-field strength of lead azide is 0.0035 V/nm. Actually, there are impurities and defects in lead azide. So, the perfect crystal can bear much stronger electric field, and we observe that the geometric and electronic structures of lead azide change somewhat when the electric field is ~0.9 V/nm. Then, the resultant electric fields applied on the crystal are 0.890, 2.674, 4.453, 6.232, and 8.017 V/nm, respectively. Note that the magnitudes of the *a*, *b*, and *c* components of the resultant field are equal, and they are 0.514, 1.542, 2.570, 3.598, and 4.626 V/nm, respectively.

Both the structural change and the Franz−Keldysh effect can cause the band gap reduction.[13] If the field is not applied in the electronic structure calculation, the band gap reduction is just induced by the structural change resulted from external electric field. The electric field must be applied not only in the geometry

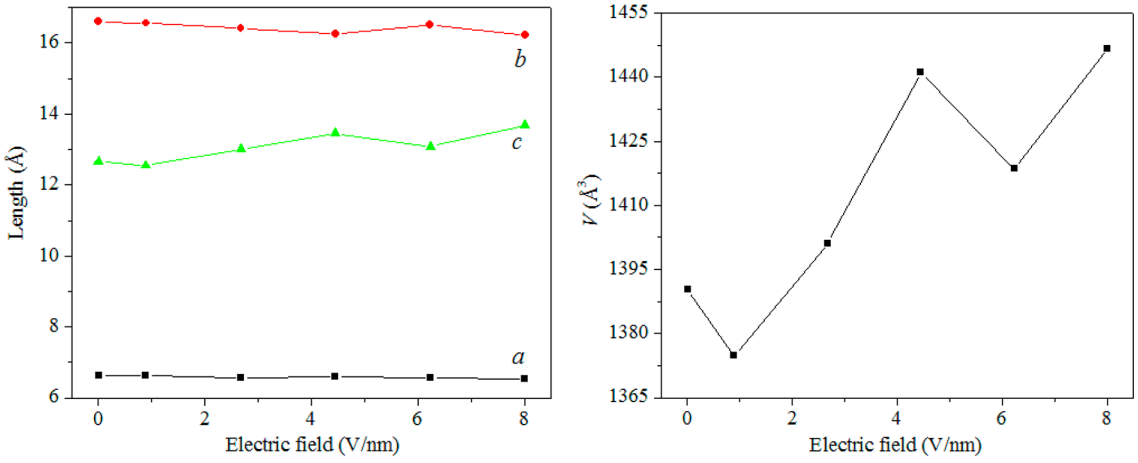

Figure 2. Calculated lengths of the crystallographic axes (*a*, *b*, and *c*) and the unit cell volume (*V*) of lead azide at different resultant electric field strengths.

DOI: 10.1021/jp507822z
J. Phys. Chem. C 2015, 119, 8431−8437

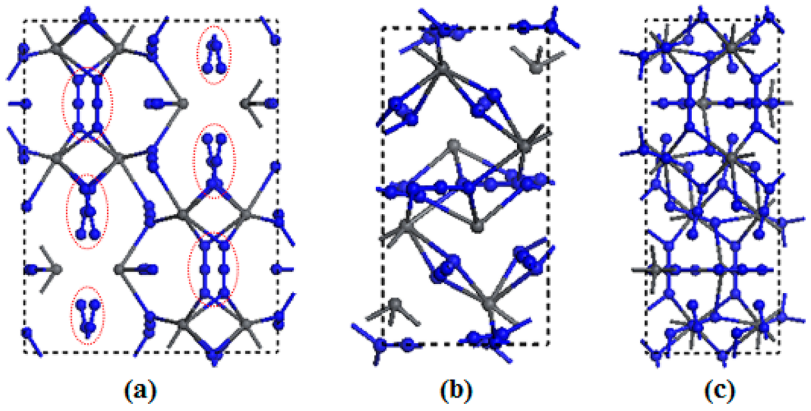

Figure 3. Perspective views of unit cell of lead azide along the *a* (a), *b* (b), and *c* (c) axes. The π-stacked dimers of azide ion are highlighted in red circle.

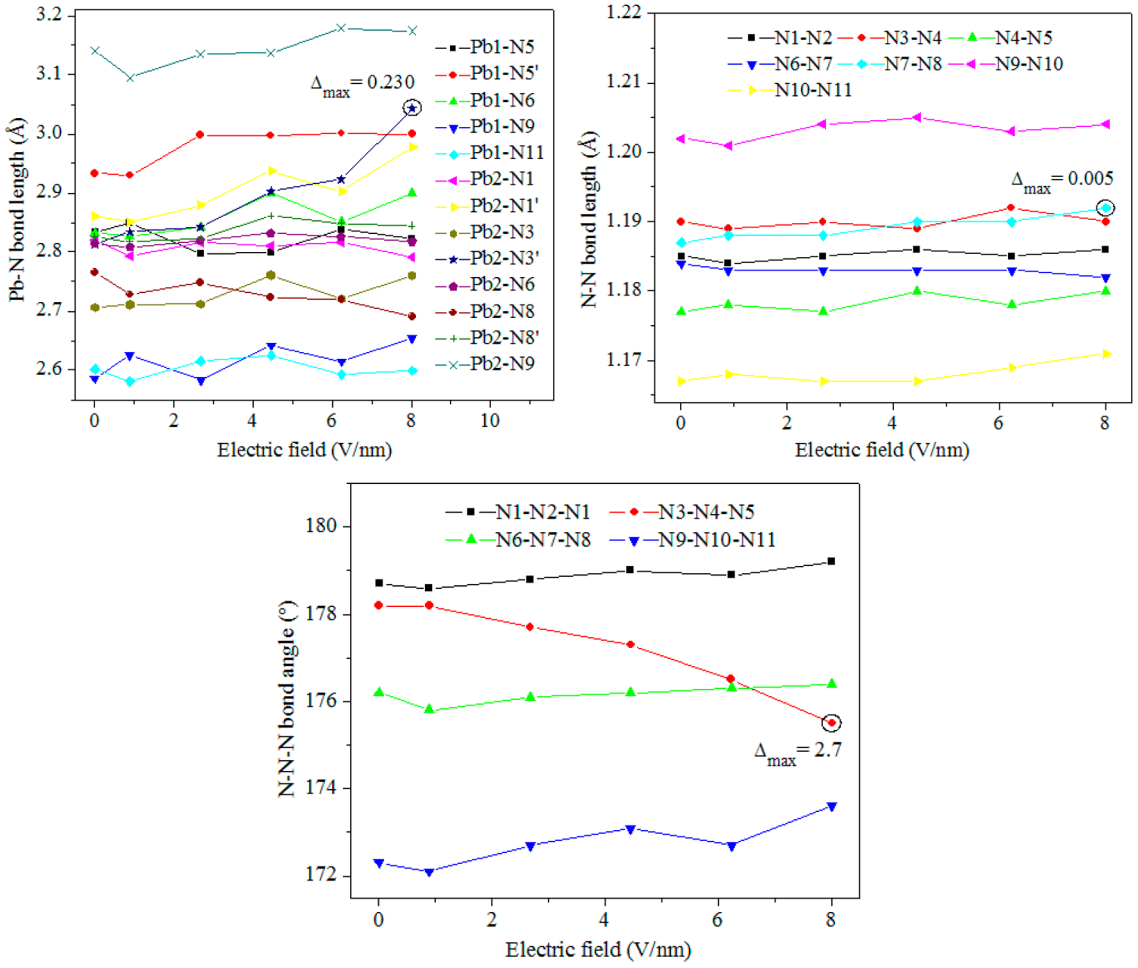

Figure 4. Variation of the Pb−N and N−N bond lengths and the N−N−N bond angles with the resultant electric field. Δ_{max} denotes the maximum variation and is marked with circle.

optimization but also in the electronic structure calculation to explore the influence of the both factors on the band gap. All density functional theoretical calculations reported in this work were carried out with the DMol^3 code,[45,46] which is incorporated into the Materials Studio (MS) software.

3. RESULTS AND DISCUSSION

3.1. Crystal Structure. To show the effect of external electric field on the crystal structure, Figure 2 displays the relaxed lattice constants (*a*, *b*, and *c*) and unit cell volume (*V*) of lead azide at applied electric fields varying from 0 to 8.017 V/nm. Note that the lattice parameters of α, β, and γ are always the same and $\alpha = \beta = \gamma = 90°$. As shown in Figure 2, there exist different variation trends along three crystallographic directions, indicating that the influence of external electric field on the structure of bulk lead azide is anisotropic. Obviously, the length of the crystallographic axis *a* almost remains constant, which reveals that lead azide is more sensitive to external electric field along the *b* and *c* axes than along the *a* axis. This can be interpreted from the perspective view of crystalline lead azide along three crystallographic

DOI: 10.1021/jp507822z
J. Phys. Chem. C 2015, 119, 8431−8437

directions in Figure 3. It is well known that azide ion has two big π bonds of 3 atoms and 4 π electrons denoted as Π_3^4. And it can be seen from Figure 3 that there are many π-stacked dimers of azide ion in the *a* direction; however, there are no π-stacked dimers of azide ion and further no π-stacked crystal packing in the *b* and *c* directions. Consequently, the intermolecular interaction along the *a* axis is the strongest, and so the effect of applied field on the crystal structure of lead azide in the *a*-direction is the weakest.

Moreover, with the increase in electric field, the unit cell volume varies arbitrarily, and the change ratios are smaller than 5%. Additionally, the crystal symmetry maintains the same orthorhombic space group *Pnma* under all field actions as the one determined experimentally. It implies that lead azide maybe merely changes its structure continuously and has no phase transition upon the external electric field in range from 0 to 8.017 V/nm.

3.2. Molecular Structure. The electric field causes the changes in not only the unit cell but also the molecular geometry. Some important geometrical parameters including bond lengths and bond angles at various electric fields are presented in Figure 4. On the whole, the variations of both the bond lengths and bond angles with external electric field are quite different. With the applied field increasing from 0 to 8.017 V/nm, some bonds elongate continuously, others shorten gradually, and still others vary arbitrarily. Clearly, most bond parameters do not monotonically change with the increasing electric field, which is similar to lead styphnate.[13]

The maximum changes of the Pb−N and N−N bond lengths are 0.230 and 0.005 Å, respectively, which occur at the electric field of 8.017 V/nm. As reported in ref 32, the N−N bonds are covalent, but Pb−N bonds are ionic in nature. Apparently, the variations of interatomic distances of the ionic bonds are much bigger than those of the covalent bonds. This is attributed to the difference in atomic charge on Pb and N atoms. According to ref 32, the effective charge of the Pb atom is 1.35, whereas that of the central N atom of the azide ion is only ~0.13 and that of the end N atom ranges from −0.34 to −0.47. This shows that the charges of the Pb and N atoms in Pb−N bonds are much bigger than those of the N atoms in N−N bonds. As is well known, the electric field force (F) is readily calculated by the following equation

$$F = qE$$

where q is the electric quantity of a point charge and E is the electric field strength. The electric field applied on the crystal is a uniform field and the atomic charge can be considered as a point charge. As a result, the electric-field force applied on the ionic Pb−N bonds is much stronger than that of the covalent N−N bonds. The consequent change in the covalent bond lengths is very little, which reveals that the electric field effects on the covalent interactions are weaker than those on the ionic interactions.

In addition, it can be seen from Figure 4 that the maximum change of the N−N−N bond angles is 2.7°, which also arises at the electric field of 8.017 V/nm. It is worthwhile to note that increasing the electric field makes the N3−N4−N5 bond angle reduce gradually, and the corresponding azide ion bend slowly.

3.3. Density of States. An analysis of density of states is very helpful to understand the changes in electronic structure caused by external electric field. Figure 5 presents the calculated total density of states for crystalline lead azide at different resultant electric field strengths. As can be easily seen, the DOS curve hardly varies at the electric field of 0.890 V/nm, indicating that

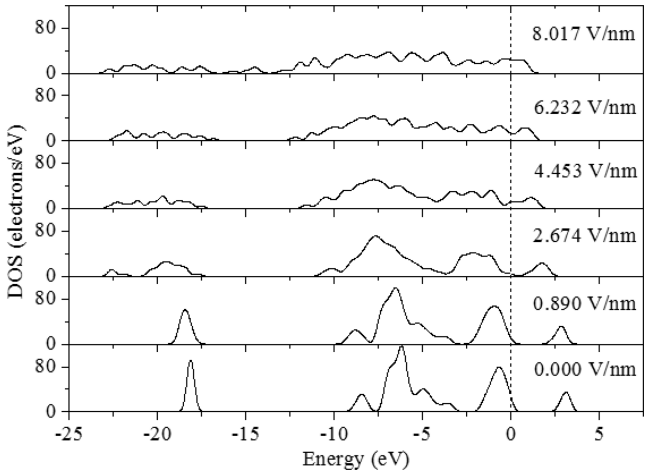

Figure 5. Total density of states (DOS) of lead azide crystal at different resultant electric field strengths.

the electronic structure of lead azide does not have any significant changes; however, in the field range from 2.674 to 8.017 V/nm, the shape of the DOS curve changes remarkably. Moreover, the applied field makes the DOS peaks split and lower, and the electron distribution is more delocalized. More interestingly, the conduction band has a tendency of shifting to the lower energy, consequently leading to a reduction in band gap. At fields higher than 4.453 V/nm, there is a band gap closure between valence and conduction bands in the system. It means that lead azide has metallic properties in the presence of an electric field above 4.453 V/nm. Such metallization has also been found to occur under heating or hydrostatic compression in other energetic materials.[4−8] The band gap lowering or closing greatly increases the probability of the electronic excitation that may cause the chemical decomposition and the final detonation of explosives.

3.4. Band Gap and Stability. The band gaps of bulk lead azide and lead styphnate ($HC_6N_3O_8Pb{\cdot}H_2O$) at different resultant electric-field strengths are shown in Figure 6. The results of lead styphnate has been previously reported.[13] Note that the electric field strength is the component in our previous report, but here the resultant electric field strength is used. Although the *a*, *b*, and *c* components are the same, the resultant

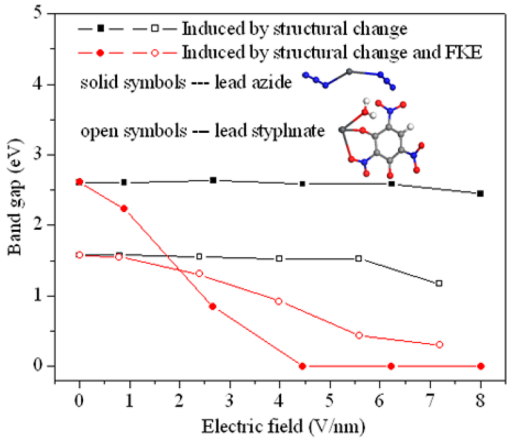

Figure 6. Variation of the band gap of lead azide and lead styphnate with the resultant electric field. The two compounds are also shown in a molecular ball and stick model. Gray, blue, red, white, and dark-gray spheres stand for C, N, O, H, and Pb atoms, respectively.

DOI: 10.1021/jp507822z
J. Phys. Chem. C 2015, 119, 8431−8437

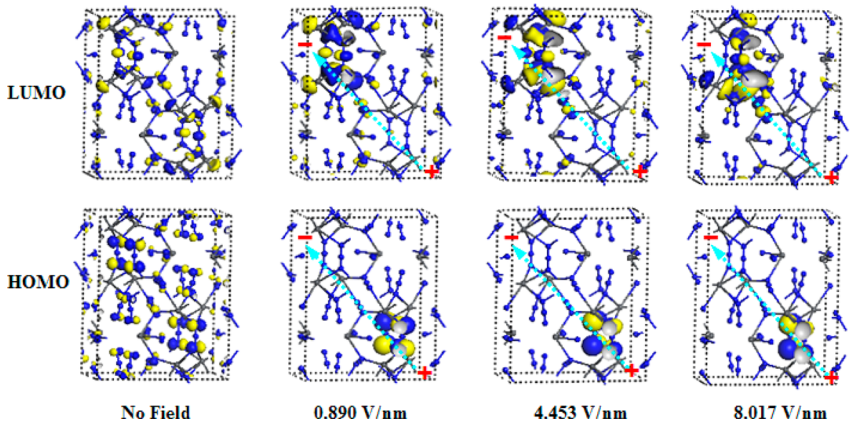

Figure 7. Evolution of the distribution of frontier molecular orbitals of lead azide as a function of the field applied. The positive and negative signs and green arrow denote the anode, cathode, and resultant field direction, respectively. Note that the applied field is spatially uniform and both electrodes are plane-shaped; the choice of anode and cathode points is arbitrary.

fields applied on lead azide and lead styphnate are not equal because the magnitudes of their lattice parameter β are different. The resultant electric fields applied on lead styphnate are 0.797, 2.396, 3.990, 5.584, and 7.184 V/nm, respectively. In the absence of the field, lead azide exhibits a small energy gap of 2.61 eV between valence and conduction bands. This value is slightly larger than the band gap of 2.42 eV using PW91 functional with ultrasoft pseudopotentials and a plane-wave basis set.[34] In comparison with experiments, band gaps are generally underestimated in density functional theoretical calculations, but these errors are close to being shifts of band energies. The magnitude of the computed band gap indicates that there may be some conductivity in crystalline lead azide. This is supported by the previous experimental result that lead azide has some electrical conductivity.[47,48] For both lead azide and lead styphnate, the band gap decreases gradually with the applied field increasing, and the effect of FKE on the band gap is greater than that of the structural change. More interestingly, as the field increases from 4.453 to 8.017 V/nm, the band gap of lead azide disappears, which differs remarkably from lead styphnate.

As is well known, band gap is an important parameter to characterize the electronic structure of solids and retains close connection to some bulk properties. Here we discuss the correlation of stabilities (or sensitivity properties) of the two crystals at different electric fields with the band gap. As depicted in Figure 6, the band gaps of the two primary explosives gradually reduce with the increment of applied field. According to the first-principles band gap criterion,[49] we can conclude that their impact sensitivity becomes more and more sensitive with the external electric field increasing. For energetic materials, the detonation initiation induced by external mechanical stimuli is taken to be an electronic excitation process.[50−53] Thus, a possible explanation may be that the increased impact sensitivity is caused by the increased number of excited states due to optical band gap reduction.

As can also be seen from Figure 6, the band gap reduction of the two systems is analogous in the case of structural change; however, the band gap reduction of lead azide is much larger than that of lead styphnate in the case of structural change and FKE. Accordingly, lead azide has a stronger Franz−Keldysh effect and is more sensitive to external electric field. In fact, the room-temperature breakdown-field strength of lead azide is 3.5 MV/m, whereas lead styphnate breaks down at the electric field of 5.5 MV/m.[36]

3.5. Frontier Molecular Orbitals and Decomposition Mechanism. The highest occupied molecular orbital (HOMO) and the lowest unoccupied molecular orbital (LUMO) are analyzed in detail and plotted in Figure 7 to further investigate the electronic change of lead azide in the presence of the electric field and its mechanism of electrical decomposition. In the absence of the field, the HOMO represents nonbonding orbital occupied by the lone-pair electrons of the end nitrogen atoms of the azide ions, and the LUMO is mainly dominated by the lead and central nitrogen atoms. As electric field acts on the system, the frontier molecular orbitals change drastically. For the HOMO orbital, electron density only localizes on two azide ions in the unit cell. Similarly, the electric field also redistributes the electron density of the LUMO orbital. That is, the LUMO is predominantly donated by the lead ions, but the nitrogen atoms make a little contribution, and the distribution reduces gradually and slowly with the increasing electric field from 0.890 to 8.017 V/nm.

In the presence of the electric field, electrons and holes were injected into the lead azide crystal from the cathode and anode, respectively. As can be easily seen from Figure 7, the HOMO orbital approaches the anode and just localizes on two azide ions under the applied field. Hence it is more favorable for an azide ion to combine with a hole than for it to combine with an electron. Their combination is represented by

$$N_3^- + h^+ \rightarrow N_3$$

where h denotes the hole. Subsequently, N_3 combines bimolecularly due to its instability and generates nitrogen gas

$$N_3 + N_3 \rightarrow 3N_2$$

On the contrary, the LUMO orbital is close to the cathode and mostly contributed from the lead ions in the presence of the electric field. Hereby it is more favorable for a lead ion to capture free electrons, and their combination may give rise to the following chemical reaction

$$Pb^{2+} + 2e^- \rightarrow Pb$$

where e stands for the electron. The proposed mechanism of electrical decomposition is supported by the previous experimental observations of the appearance of metallic lead on the crystal surface and the evolution of nitrogen gas.[35] In the absence of the field, the thermal excitation of electrons from HOMO to LUMO can also result in the aforementioned chemical reactions

DOI: 10.1021/jp507822z
J. Phys. Chem. C 2015, 119, 8431−8437

because the composition of the frontier molecular orbitals of lead azide is almost identical in the presence and absence of the electric field. It is clear that the main difference in the process of thermal and electrical decompositions is responsible for the generation of electrons and holes, which is thermal excitation in the thermal case but field injection in the electrical case.

4. CONCLUSIONS

We have performed a detailed theoretical study of electric field effects on the structure, decomposition mechanism, and stability of crystalline lead azide. The obtained results show that the influence of external electric field on the crystal structure is anisotropic due to the difference in crystal packing along three crystallographic directions. Lead azide has a little change in unit cell volume and always belongs to orthorhombic *Pnma* space group, revealing that there could be simply a continuous change in structure and no phase transition occurs under the applied field. The electric field effects on the ionic interactions are stronger than those on the covalent interactions because of more atomic charges on the composing atoms of the ionic bonds. Lead azide possesses metallic properties at the field higher than 4.453 V/nm. Furthermore, the Franz−Keldysh effect can yield greater influence on the band gap than the structural change, and lead azide is more sensitive to external electric field than lead styphnate. As electric field acts on lead azide crystal, the distribution of frontier molecular orbitals reduces evidently, but their composition varies slightly. Thus, the thermal excitation of electrons from HOMO to LUMO and both orbitals combining with holes and electrons injected by the applied field may lead to the same chemical reactions; the mechanism of electrical and thermal decompositions is similar. In addition, the electrical decomposition of lead azide produces nitrogen gas and metallic lead.

AUTHOR INFORMATION

Corresponding Authors

*H.H.: E-mail: h.s.huang@hotmail.com. Tel/Fax: (86)-10-6891-1202.

*T.Z.: E-mail: ztlbit@bit.edu.cn.

Author Contributions

‖H.H. and Z.L. contributed equally.

Notes

The authors declare no competing financial interest.

ACKNOWLEDGMENTS

This work was supported by the China National "973" project, the Chunhui Program of Ministry of Education of China (Z2014083, Z2014084), the Natural Science Foundation of Chongqing (cstc2011jjA50013), the Fuling Science and Technology Commission (FLKJ2014ABA2022), and the Young Talented Researcher Plan of Yangtze Normal University (2014QNRC03).

REFERENCES

(1) Franz, W. Einflus eines Elektrischen Feldes auf eine Optische Absorptionskante. *Z. Naturforsch.* **1958**, *13a*, 484−489.

(2) Keldysh, L. V. Behaviour of Non-metallic Crystals in Strong Electric Fields. *J. Exp. Theor. Phys.* **1957**, *33*, 994−1003.

(3) Behler, K. D.; Ciezak-Jenkins, J. A.; Sausa, R. C. High-Pressure Characterization of Nitrogen-Rich Bis-Triaminoguanidinium Azotetrazolate (TAGzT) by in Situ Raman Spectroscopy. *J. Phys. Chem. A* **2013**, *117*, 1737−1743.

(4) Xu, X. J.; Zhu, W. H.; Xiao, H. M. DFT Studies on the Four Polymorphs of Crystalline CL-20 and the Influences of Hydrostatic Pressure on ε-CL-20 Crystal. *J. Phys. Chem. B* **2007**, *111*, 2090−2097.

(5) Qiu, L.; Zhu, W. H.; Xiao, J. J.; Xiao, H. M. Theoretical Studies of Solid Bicyclo-HMX: Effects of Hydrostatic Pressure and Temperature. *J. Phys. Chem. B* **2008**, *112*, 3882−3893.

(6) Liu, Y.; Gong, X. D.; Wang, L. J.; Wang, G. X. Effect of Hydrostatic Compression on Structure and Properties of 2-Diazo-4,6-Dinitrophenol Crystal: Density Functional Theory Studies. *J. Phys. Chem. C* **2011**, *115*, 11738−11748.

(7) Liu, Y.; Zhang, L.; Wang, G. X.; Wang, L. J.; Gong, X. D. First-Principle Studies on the Pressure-Induced Structural Changes in Energetic Ionic Salt 3-Azido-1,2,4-Triazolium Nitrate Crystal. *J. Phys. Chem. C* **2012**, *116*, 16144−16153.

(8) Zhu, W. H.; Xiao, H. M. Ab Initio Molecular Dynamics Study of Temperature Effects on the Structure and Stability of Energetic Solid Silver Azide. *J. Phys. Chem. C* **2011**, *115*, 20782−20787.

(9) Ge, N. N.; Wei, Y. K.; Ji, G. F.; Chen, X. R.; Zhao, F.; Wei, D. Q. Initial Decomposition of the Condensed-Phase β-HMX under Shock Waves: Molecular Dynamics Simulations. *J. Phys. Chem. B* **2012**, *116*, 13696−13704.

(10) Manaa, M. R.; Fried, L. E. Nearly Equivalent Inter- and Intramolecular Hydrogen Bonding in 1,3,5-Triamino-2,4,6-Trinitrobenzene at High Pressure. *J. Phys. Chem. C* **2012**, *116*, 2116−2122.

(11) Pravica, M.; Liu, Y.; Robinson, J.; Velisavljevic, N.; Liu, Z. X.; Galley, M. A High-Pressure Far- and Mid-Infrared Study of 1,1-Diamino-2,2-Dinitroethylene. *J. Appl. Phys.* **2012**, *111*, 103534.

(12) Pravica, M.; Galley, M.; Park, C.; Ruiz, H.; Wojno, J. A High Pressure, High Temperature Study of 1,1-Diamino-2,2-Dinitro Ethylene. *High Pressure Res.* **2011**, *31*, 80−85.

(13) Li, Z.; Huang, H.; Zhang, T.; Zhang, S.; Zhang, J.; Yang, L. First-Principles Study of Electric Field Effects on the Structure, Decomposition Mechanism, and Stability of Crystalline Lead Styphnate. *J. Mol. Model.* **2014**, *20*, 2072−2079.

(14) Auzanneau, M.; Roux, M. Electric Spark and ESD Sensitivity of Reactive Solids, Part II: Energy Transfer Mechanism and Comprehensive Study on E_{50}. *Propellants, Explos., Pyrotech.* **1995**, *20*, 96−101.

(15) Skinner, D.; Olson, D.; Block-Bolten, A. Electrostatic Discharge Ignition of Energetic Materials. *Propellants, Explos., Pyrotech.* **1997**, *23*, 34−42.

(16) Talawar, M. B.; Agrawal, A. P.; Anniyappan, M.; Wani, D. S.; Bansode, M. K.; Gore, G. M. Primary Explosives: Electrostatic Discharge Initiation, Additive Effect and Its Relation to Thermal and Explosive Characteristics. *J. Hazard. Mater.* **2006**, *137*, 1074−1078.

(17) Badgujar, D. M.; Talawar, M. B.; Asthana, S. N.; Mahulikar, P. P. Advances in Science and Technology of Modern Energetic Materials: An Overview. *J. Hazard. Mater.* **2008**, *151*, 289−305.

(18) Talawar, M. B.; Sivabalan, R.; Mukundan, T.; Muthurajan, H.; Sikder, A. K.; Gandhe, B. R.; Rao, A. S. Environmentally Compatible Next Generation Green Energetic Materials (GEMs). *J. Hazard. Mater.* **2009**, *161*, 589−607.

(19) Zhi, C.; Cheng, X.; Zhao, F. The Correlation between Electric Spark Sensitivity of Polynitroaromatic Compounds and their Molecular Electronic Properties. *Propellants, Explos., Pyrotech.* **2010**, *35*, 555−560.

(20) Zhi, C.; Cheng, X.; Zhao, F. Relationship between Electric Spark Sensitivity of Cyclic Nitramines and Their Molecular Electronic Properties. *Chin. J. Struct. Chem.* **2012**, *31*, 1263−1270.

(21) Türker, L. Contemplation on Spark Sensitivity of Certain Nitramine Type Explosives. *J. Hazard. Mater.* **2009**, *169*, 454−459.

(22) Zeman, S. New Aspects of Initiation Reactivities of Energetic Materials Demonstrated on Nitramines. *J. Hazard. Mater.* **2006**, *132*, 155−164.

(23) Zeman, S.; Pelikan, V.; Majzlik, J. Electric Spark Sensitivity of Nitramines. Part I. Aspects of Molecular Structure. *Cent. Eur. J. Energy Mater.* **2006**, *3*, 27−44.

(24) Zeman, V.; Koci, J.; Zeman, S. Electric Spark Sensitivity of Polynitro Compounds. Part II. A Correlation with Detonation Velocities of Some Polynitro Arenas. *Chin. J. Energy Mater.* **1999**, *7*, 127−132.

DOI: 10.1021/jp507822z
J. Phys. Chem. C 2015, 119, 8431−8437

(25) Zeman, V.; Koci, J.; Zeman, S. Electric Spark Sensitivity of Polynitro Compounds. Part III. A Correlation with Detonation Velocities of Some Nitramines. *Chin. J. Energy Mater.* **1999**, *7*, 172−175.
(26) Zeman, S.; Koci, J. Electric Spark Sensitivity of Polynitro Compounds. Part IV. A Relation to Thermal Decomposition Parameters. *Chin. J. Energy Mater.* **2000**, *8*, 18−26.
(27) Koci, J.; Zeman, V.; Zeman, S. Electric Spark Sensitivity of Polynitro Compounds. Part V. A Relationship Between Electric Spark and Impact Sensitivities of Energetic Materials. *Chin. J. Energy Mater.* **2001**, *9*, 60−65.
(28) Keshavarz, M. H.; Pouretedal, H. R.; Semnani, A. Reliable Prediction of Electric Spark Sensitivity of Nitramines: A General Correlation with Detonation Pressure. *J. Hazard. Mater.* **2009**, *167*, 461−466.
(29) Keshavarz, M. H. Theoretical Prediction of Electric Spark Sensitivity of Nitroaromatic Energetic Compounds Based on Molecular Structure. *J. Hazard. Mater.* **2008**, *153*, 201−206.
(30) Keshavarz, M. H.; Pouretedal, H. R.; Semnani, A. A Simple Way to Predict Electric Spark Sensitivity of Nitramines. *Indian J. Eng. Mater. Sci.* **2008**, *15*, 505−509.
(31) Keshavarz, M. H. Relationship between the Electric Spark Sensitivity and Detonation Pressure. *Indian J. Eng. Mater. Sci.* **2008**, *15*, 281−286.
(32) Choi, C. S.; Prince, E.; Garrett, W. L. Refinement of Alpha-Lead Azide by Neutron Diffraction. *Acta Crystallogr., Sect. B* **1977**, *33*, 3536−3537.
(33) Evans, B. L.; Yoffe, A. D.; Gray, P. Physics and Chemistry of the Inorganic Azides. *Chem. Rev.* **1959**, *59*, 515−568.
(34) Zhu, W. H.; Xiao, H. M. Ab Initio Study of Energetic Solids: Cupric Azide, Mercuric Azide, and Lead Azide. *J. Phys. Chem. B* **2006**, *110*, 18196−18203.
(35) Tang, T. B.; Chaudhri, M. M. Dielectric Breakdown by Electrically Induced Chemical Decomposition. *Nature* **1979**, *282*, 54−55.
(36) Cai, R. J. *The Design Principle for Initiating Explosive Devices*; Beijing Institute of Technology Press: Beijing, 1999.
(37) Wang, L.; Zhang, Y. Z.; Zhang, Y. F.; Chen, X. S.; Lu, W. Electronic Structures of S-Doped Capped C-SWNT from First Principles Study. *Nanoscale Res. Lett.* **2010**, *5*, 1027−1031.
(38) Baei, M. T.; Peyghan, A. A.; Moghimi, M. Electric Field Effect on (6,0) Zigzag Single-Walled Aluminum Nitride Nanotube. *J. Mol. Model.* **2012**, *18*, 4477−4489.
(39) Baei, M. T.; Peyghan, A. A.; Moghimi, M.; Hashemian, S. Electric Field Effect on the Zigzag (6,0) Single-Wall BC_2N Nanotube for Use in Nano-Electronic Circuits. *J. Mol. Model.* **2013**, *19*, 97−107.
(40) Chattopadhyaya, M.; Alam, M. M.; Chakrabarti, S. On the Microscopic Origin of Bending of Graphene Nanoribbons in the Presence of a Perpendicular Electric Field. *Phys. Chem. Chem. Phys.* **2012**, *14*, 9439−9443.
(41) Jissy, A. K.; Datta, A. Effect of External Electric Field on H-Bonding and π-Stacking Interactions in Guanine Aggregates. *ChemPhysChem* **2012**, *13*, 4163−4172.
(42) Calvaresi, M.; Martinez, R. V.; Losilla, N. S.; Martinez, J.; Garcia, R.; Zerbetto, F. Splitting CO_2 with Electric Fields: A Computational Investigation. *J. Phys. Chem. Lett.* **2010**, *1*, 3256−3260.
(43) Zhu, W. H.; Xiao, J. J.; Xiao, H. M. Density Functional Theory Study of the Structural and Optical Properties of Lithium Azide. *Chem. Phys. Lett.* **2006**, *422*, 117−121.
(44) Perdew, J. P.; Chevary, J. A.; Vosko, S. H.; Jackson, K. A.; Pederson, M. R.; Singh, D. J.; Fiolhais, C. Atoms, Molecules, Solids, and Surfaces: Applications of the Generalized Gradient Approximation for Exchange and Correlation. *Phys. Rev. B* **1992**, *46*, 6671−6687.
(45) Delley, B. An All-Electron Numerical-Method for Solving the Local Density Functional for Polyatomic-Molecules. *J. Chem. Phys.* **1990**, *92*, 508−517.
(46) Delley, B. From Molecules to Solids with the $DMol^3$ Approach. *J. Chem. Phys.* **2000**, *113*, 7756−7764.
(47) Urbanski, T. *Chemistry and Technology of Explosives*; Pergamon: London, 1967.
(48) Savelev, G. G.; Zakharov, Y. A.; Shechkov, G. T. Systems Lead Azide (PbN6)-Silver Azide (AgN3) and Lead Azide (PbN6)-Copper Azide (CuN6) with a High Lead Azide Content. *Russ. J. Phys. Chem.* **1967**, *41*, 904−908.
(49) Zhu, W. H.; Xiao, H. M. First-Principles Band Gap Criterion for Impact Sensitivity of Energetic Crystals: A Review. *Struct. Chem.* **2010**, *21*, 657−665.
(50) Kuklja, M. M.; Stefanovich, E. V.; Kunz, A. B. An Excitonic Mechanism of Detonation Initiation in Explosives. *J. Chem. Phys.* **2000**, *112*, 3417−3423.
(51) Kuklja, M. M.; Kunz, A. B. Compression-Induced Effect on the Electronic Structure of Cyclotrimethylene Trinitramine Containing an Edge Dislocation. *J. Appl. Phys.* **2000**, *87*, 2215−2218.
(52) Luty, T.; Ordon, P.; Eckhardt, C. J. A Model for Mechanochemical Transformations: Applications to Molecular Hardness, Instabilities, and Shock Initiation of Reaction. *J. Chem. Phys.* **2002**, *117*, 1775−1785.
(53) Faust, W. L. Explosive Molecular Ionic Crystals. *Science* **1989**, *245*, 37−42.

DOI: 10.1021/jp507822z
J. Phys. Chem. C 2015, 119, 8431−8437